Antiproton portable traps and medical applications[*]

R.A. Lewis and G. A. Smith
Department of Physics
Pennsylvania State University
University Park, PA 16802

S.D. Howe
Los Alamos National Laboratory
Los Alamos, NM 87545

Several medical applications utilizing antiprotons stored and transported in a portable Penning trap are considered. These include production of radioisotopes for PET, radiography and radiotherapy. Specifications of a portable antiproton trap suitable for this work are discussed, and progress on the development of such a trap is reported.

1.   Introduction

Trapping of large numbers of antiprotons has made great strides in the past few years, witness papers presented at this workshop [1,2]. Because of the myriad interests expressed in low energy antiprotons at this workshop, e.g. basic experiments in atomic physics, antimatter gravity, and antihydrogen physics, it seems natural that the use of portable traps would be considered. This would facilitate distribution of the valuable antiprotons from the central production site, i.e. CERN or Fermilab, to interested parties worldwide, including smaller and remote research laboratories where students could benefit first-hand from this work. It could also make the conditions for doing precision experiments with antiprotons, e.g. spectroscopy of atomic antihydrogen, much improved over those experienced at the production sites [3].

Certain important and accepted medical applications could be made more available and/or effective using antiprotons delivered to clinics in portable traps. This presentation illustrates some of these applications, and attempts to show how they can be carried out in a practical and cost-effective way. We conclude by describing the progress currently being made in the development of such a portable trap.

2.   Medical applications

We outline two medical applications of a portable antiproton trap. These are (a) a radioisotope generator for Positron Emission Tomography (PET), and (b) radiography for detection and ultimate treatment (radiotherapy) of tumors. In both instances, we have focused on applications where currently available numbers of antiprotons could make a serious impact, and where clinical results and/or availability could be significantly improved over techniques currently being used in

---

these areas.

2.1 An antiproton portable radioisotope generator for PET

The four most important PET isotopes are radioactive species of carbon, nitrogen, oxygen and fluorine ([4], see Table 1). Their decay lifetimes range from several minutes to less than two hours, making it essential that they be produced by an accelerator (current method), or portable antiproton trap (proposed method) located close to the PET scanner. The nuclear reactions shown in Table 1 (current method) or antiproton annihilation (proposed method discussed later) are responsible for the production of the desired radioisotope.

Table 1. Important PET isotopes, lifetimes, cyclotron production reactions, radio-pharmaceuticalapplications and diagnostic uses [4].

Isotope	Halflife (min)	Production Reactions	Radio-pharmaceutical	Diagnostic Use
C^{11}	20	$N^{14}(p,\alpha)C^{11}$	C^{11} methylspiperone C^{11} acetate C^{11} methionine	dopamine binding cardiac metabolism amino acid metabolism
N^{13}	10	$O^{16}(p,\alpha)N^{13}$ $O^{13}(p,n)N^{13}$	N^{13} ammonia	cardiac blood flow
O^{15}	2	$N^{14}(d,n)O^{15}$ $N^{15}(p,n)O^{15}$	O^{15} water	brain blood flow
F^{18}	110	$O^{18}(p,n)F^{18}$ $Ne^{20}(d,\alpha)F^{18}$	F^{18} 2-deoxy-2 fluoro-D-glucose (FDG) F^{18} L-dopa	glucose metabolism dopamine synthesis

Radiopharmaceuticals, which are the molecules labeled by these isotopes, are put to a variety of diagnostic uses, as illustrated in Table 1. They direct the radioisotope to sites in the human body based on chemical affinity. The radioisotope emits a positron, which annihilates into two 511 keV photons after migrating one mm or so from the decay site. After several thousand back-to-back photon pairs are detected, an image of the decay site can be constructed.

Figure 1 shows a series of images of a normal brain, generated by the injection of 7 mCi of F^{18} DG into the patient on a rotating PET scanner [5]. This technique, where available, has become commonplace in the diagnosis of abnormalities of the brain, such as tumors, as well as other maladies such as epilepsy, Alzheimer's Disease, and dyslexia. Whereas x-ray CT imaging provides accurate density profiles, PET provides profiles linked to chemical uptake and related organ function.

The number of disorders and clinical treatments using PET is increasing rapidly. Far too few institutions in the US have cyclotrons to make PET isotopes to satisfy the growing demand. Further, these cyclotrons cost several $M each, which severely restricts the number and geographical distribution of PET centers. The solution to this problem is to develop a portable source, analogous to the Mo^{99} generator used as a source of Tc^{99} gamma-ray emitting isotopes.
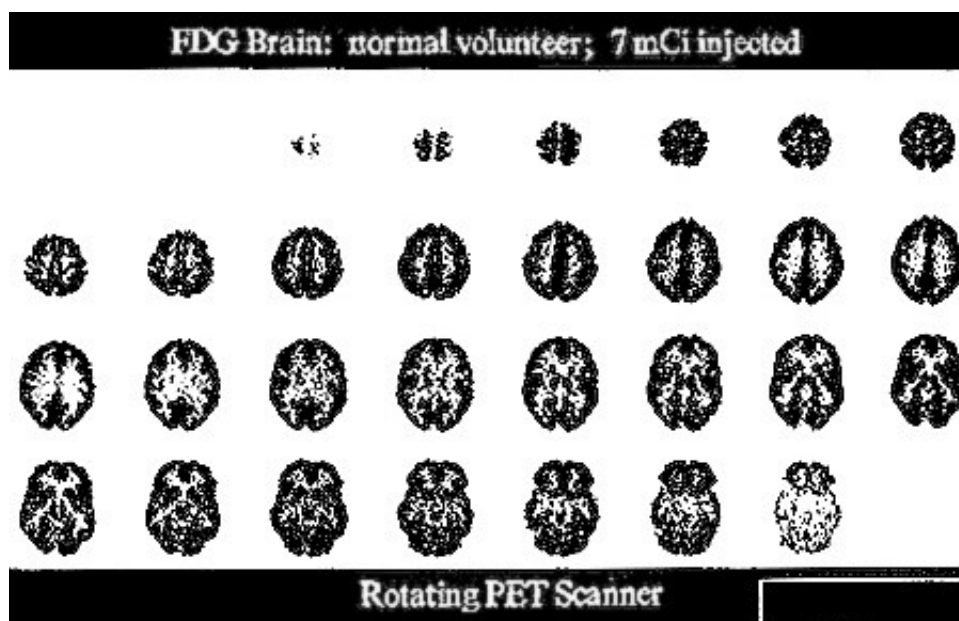
Fig. 1. Imaging the utilization of glucose in the brain by the BGO-based PET scanner at Geneva University Hospital [5].

Figure 2 shows a sketch of a portable antiproton radioisotope generating trap. It illustrates the holding of < 12 eV antiprotons, and their extraction into a water or liquid oxygen (for O^{15} production) target with a magnetic pinch coil for confinement of charged pions. Primary production by annihilation on a neutron in O^{16}, followed by internuclear production in other O^{16} nuclei due to gamma-rays, neutrons and charged pions generated in the primary interaction, are indicated. The circulation of charged pions through the target produces the majority of the O^{15}.
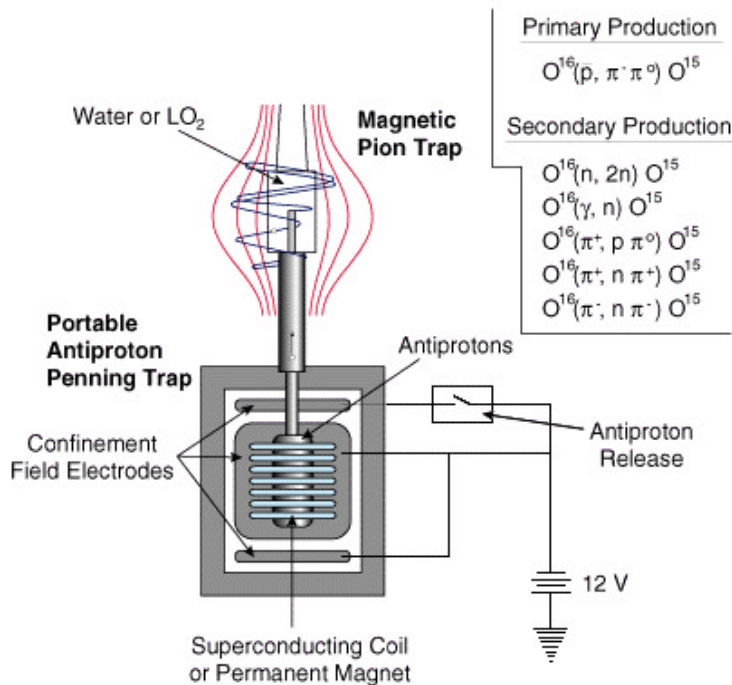

Fig.2. Portable antiproton trap for production of short-lived radionuclides (e.g., O^{15}) for positron emission tomography (PET).

Table 2. Comparison of cyclotron and antiproton trap sources of O^{15}.

Source	Yield	Comment
Cyclotron*	Saturation limit of 8 mCi per microampere reached in 2 min [4].	Available at research hospitals only.
Antiprotons	Instantaneous yield of 200 mCi per hour of Fermilab production in 1998.	Distributive system using traps, available anywhere with PET facilities.

_____
*$N^{14}(d,n)O^{15}$ @ 8 MeV

Table 2 compares the production of O^{15} by cyclotrons and portable antiproton traps. Presently, Fermilab stores 10^{11} antiprotons per hour [6]. It is further assumed that in 1998, with the operation of the Main Injector presently under construction at Fermilab, 10^{12} antiprotons will be stored per hour of beam operation. Roughly speaking, a cyclotron operated at one microampere current and an antiproton portable trap filled with 10^{12} antiprotons can each produce about 200 mCi of O^{15} per hour. With a lifetime of the antiprotons in the trap of 4-10 days, the distinct advantage of the portable trap is that it can be transported to any clinic outfitted to do PET scanning by means of commercial air or ground transportation services.

Table 3 is an attempt to estimate the cost of producing O^{15}. Since Fermilab is a very large and fully capitalized facility, it does not make sense to reproduce it. Rather, one should "rent" time, estimated by ourselves at $10K per hour. Since the high energy program does not run full-time, this appears to make a great deal of sense. With these assumptions, we estimate the cost of 1 mCi of O^{15} at $50, which we judge does not far exceed the cost of cyclotron-produced O^{15} at this time.

Table 3. Antiproton Cost Estimates (Fermilab).

	Unit Cost
I. Antiprotons/$	
a) One hour of beam ($10K) yielding 10^{12} pbars (Main Injector)	100M pbars/$
b) Independent check: L. Krauss [7] (pre-Main Injector)	20M/$
II. $/mCi (I.a)	$50/mCi

2.2   Antiproton radiotherapy and radiography

Proton radiotherapy (and radiography) are rapidly advancing fields, with currently 16 facilities worldwide treating 14,000 patients annually [8]. Antiprotons offer the primary advantage of protons, namely efficient deposition of energy at the end of their range. In addition, the annihilation mechanism which occurs when the antiproton stops provides unique and valuable assets in the task of treating (and imaging) tumors. These assets include more efficient and precise dose deposition, and the ability
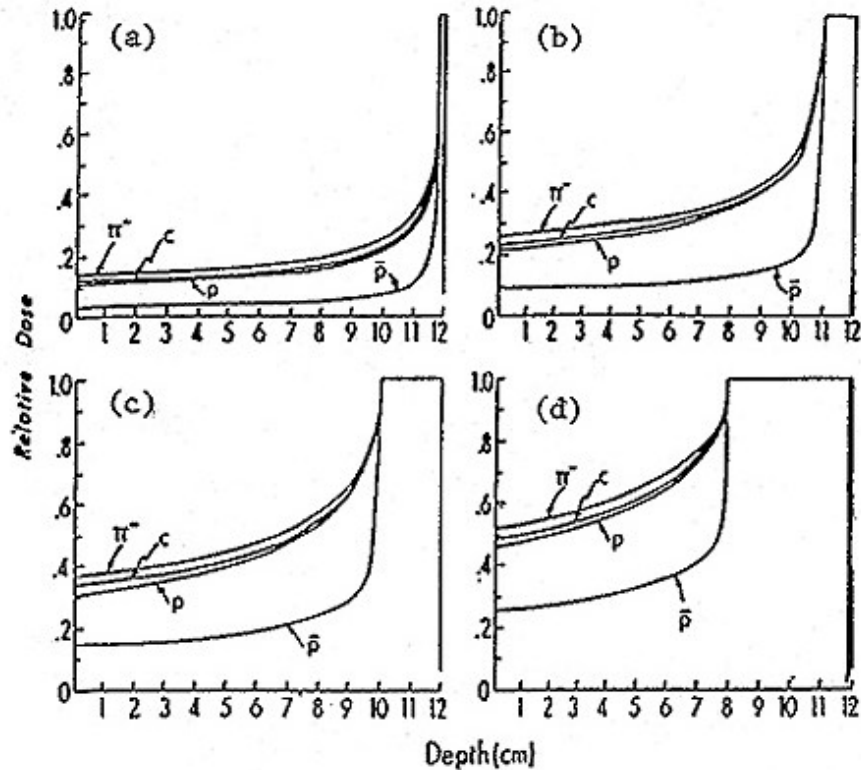
Fig. 3. Dose distributions with various ($\pi-$, p, C, $\bar{p}$) charged particle beams are compared. In computer simulations, a uniform dose was delivered to the region of a "tumor" located at a depth of 12 cm and of thickness (a) 0.3 (b) 1.0 (c) 2.0 and (d) 4.0 cm. The dose beyond 12 cm decreases rapidly and is not shown [9].

to monitor the process in real time using annihilation information.

Figure 3 illustrates the first advantage of antiprotons over protons. It shows computed stopping profiles for antiprotons, and other particles used in radiotherapy [9]. Because of the unique annihilation mechanism, the antiproton profile is much more concentrated at the end of its range, the so-called Bragg peak. Figure 4 shows actual data taken at LEAR at CERN [10]. The effectiveness of energy deposition by antiprotons at the end of their range compared to protons is striking.

This feature would enhance accurate placement of dose in radiotherapy procedures. We estimate that 10^{10} antiprotons injected into a patient at 200 MeV and stopped in a 10 gram brain tumor would render a dose of approximately 25 GYE (Gray Equivalent). This is comparable to proton treatment plans discussed in the literature [11]. We have assumed an RBE (Relative Biological Enhancement) factor of 5 (the same as protons), which is an underestimate since charged pions, gamma-rays and nuclear fragments from antiproton annihilation also deposit energy into the tumor.

The second advantage of antiprotons is that the annihilation at the end of the range produces three (on average) highly penetrating charged pions, which can be readily detected external to the patient (Fig. 5). Because the pions are emitted isotropically, the stopping point can be very accurately imaged in three dimensions and in real time, allowing more accurate and rapid diagnosis of tumor development than available with proton radiography. Figure 6 shows simulated images of a phantom, indicating sub-mm resolution in depth achieved with less than one million antiprotons [9].

Presently, the accuracy with which stopping proton beams can be placed is typically a few mm of depth. New methods are being explored in terms of achieving greater accuracy in proton
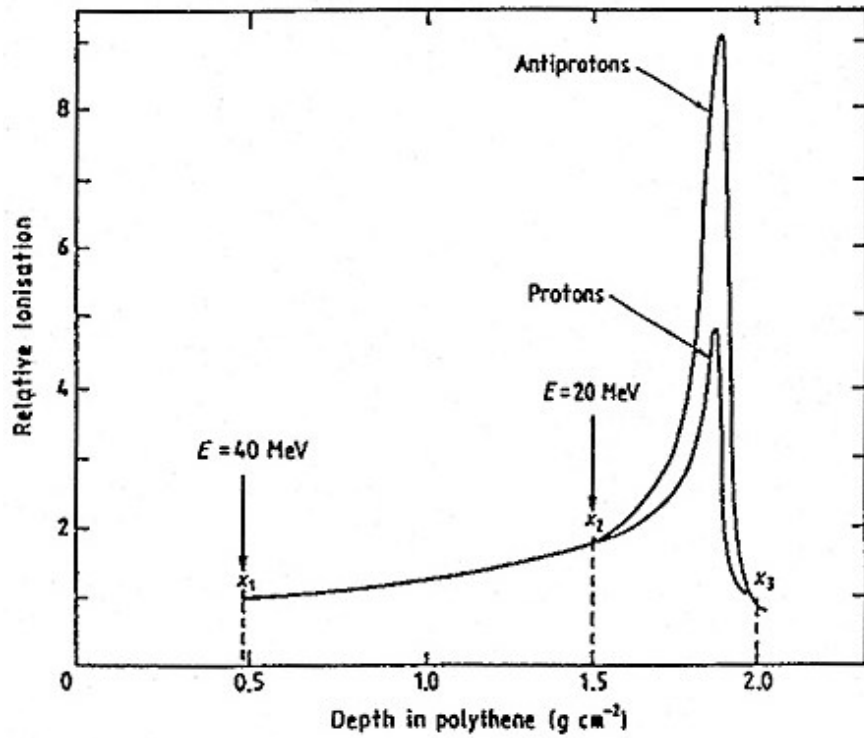
Fig. 4. Variation of energy deposition by beams of protons and antiprotons with depth in an absorber. Each curve normalized to 1 at a depth of 0.5 g cm^{-2} [10].
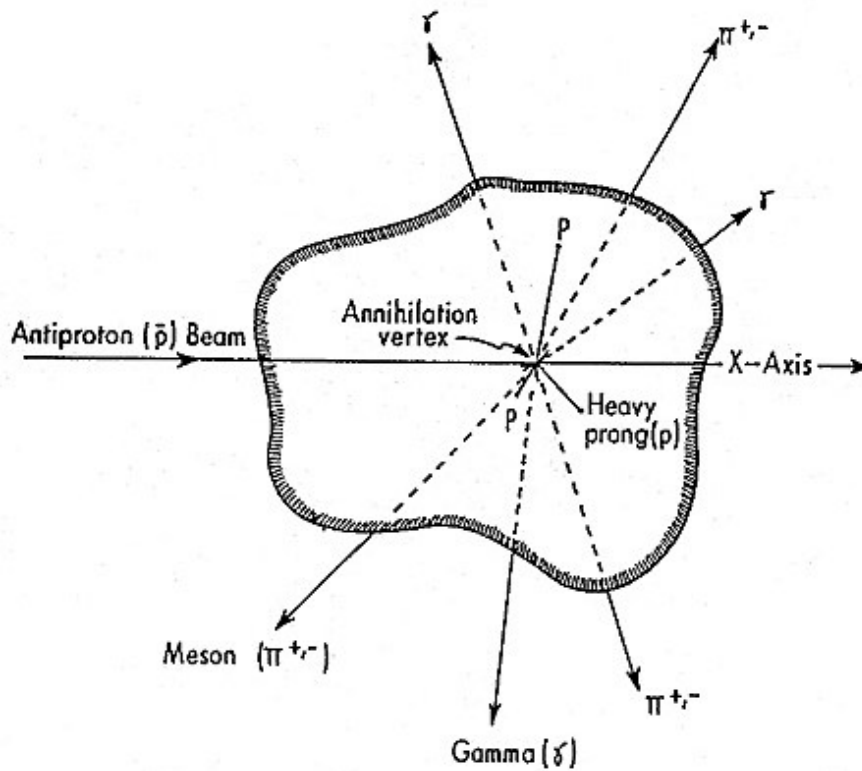

Fig. 5. Antiproton annihilation in human tissue, releasing charged pions ($\pi^{\pm}$), gamma-rays (γ), and nuclear fragments [9].
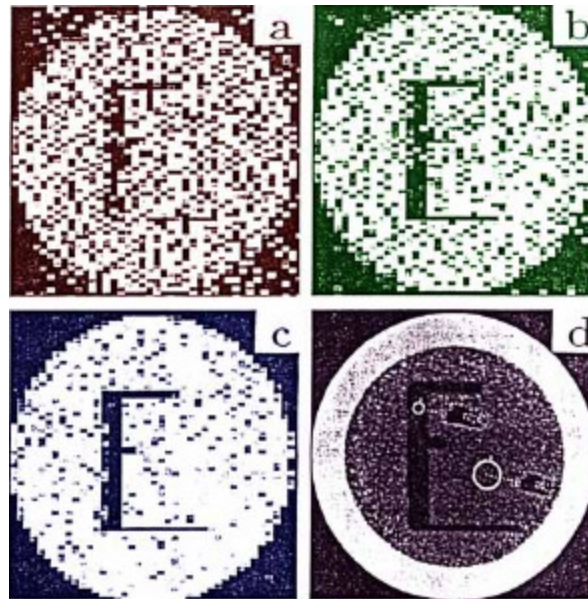
Fig. 6. (a) Simulated antiproton image of a water-lucite phantom using about 30 000 antiprotons. No "smoothing" of image has been applied. The phantom is a 3 mm thick disk of lucite in which a 1.5 mm engraving of the letter E has been made. The lucite disk is immersed in water. The phantom is 10 cm in diameter. Black represents a density of 1.15 g/cm^3. (b) Like (a) but with about 100 000 antiprotons. (c) Like (a) but with about 400 000 antiprotons. (d) This is a photograph of an actual X-ray CT scan of the phantom described in (a). The parameters of the scan and the dose are typical of head scans [9].
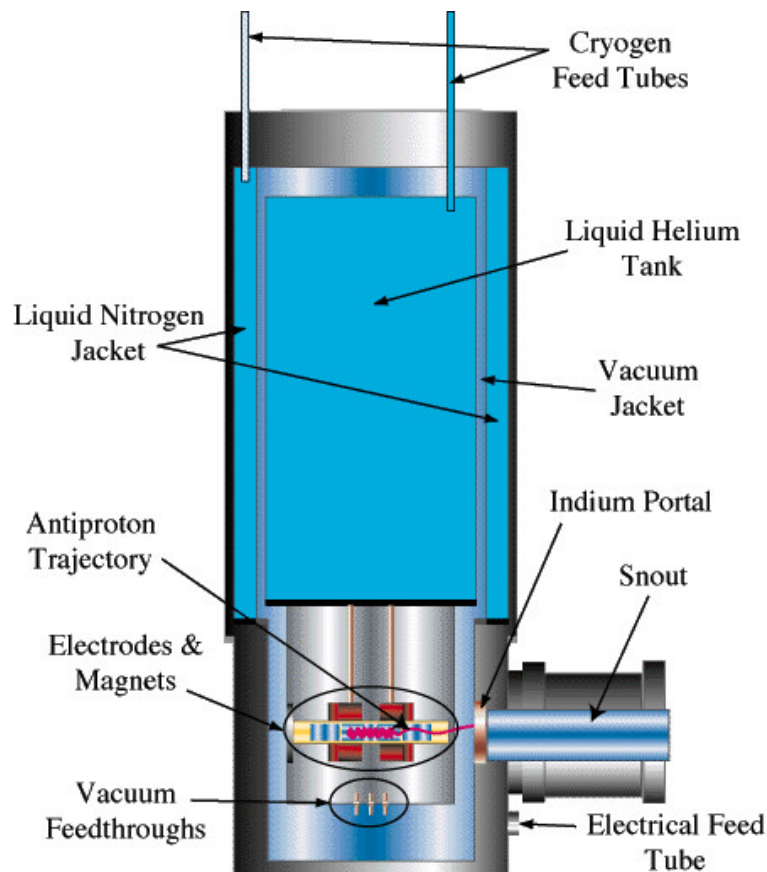

Fig. 7. Portable Penning trap.

radiotherapy procedures. Proton radiography is being studied as a means of confirming and reinforcing standard x-ray CT treatment methodology [12]. Also, proton dose monitoring using PET techniques is being investigated for the same purpose [13]. Relative to standards offered by these technologies, in our opinion antiproton radiotherapy and radiography appear to be very promising in terms of significantly improving the precision of dose deposition.

3.   Portable antiproton trap

The first portable trap will be capable of transporting about 10^{10} antiprotons. The medical applications given above could all be demonstrated feasible with this number of antiprotons. Subsequent models should carry 10^{12} antiprotons maximum. This would allow a full program of clinical PET, antiproton radiography and radiotherapy applications. The trap should have a holding time against annihilation with residual gas atoms of at least four days. This would allow commercial delivery of a full trap to a clinic anywhere in the world. For radiography and radiotherapy, development of injection into H- accelerators must proceed at the same time.

A schematic drawing of the portable trap under construction at Penn State University is shown in Fig. 7. It is 100 cm tall by 30 cm across, and weighs 55 kg fully loaded. The upper two-thirds of the trap is a cryogenic storage vessel for liquid nitrogen and helium. By conductive cooling at 4K, the lower chamber maintains a vacuum pressure of about 10^{-15} Torr, which is required for a 4 day holding time [14].

The magnet/electrode structure is held to the cryostat by a conducting copper frame support. Permanent SmCo magnets have been used and provide an axial magnetic field of 0.5 T. This results

Fig. 8. Portable antiproton trap during testing.

in a Brillouin density limit of about $10^9/cm^3$ [14]. The 10 cm^3 central volume of the trap is therefore capable of holding 10^{10} antiprotons. Antiprotons are injected through the snout, where they are trapped axially by 1 kV end electrode potentials and radially by the magnetic field. Electron cooling reduces the antiproton energy to a few hundred meV, where all systems in the portable mode can be supported by 12 V batteries.

Ejection is achieved by lowering the voltage on the end electrode nearest the snout, and gently accelerating the antiprotons through the snout to about 1 keV energy by use of einzel lenses. A recent photograph of the trap during initial pump-down exercises is shown in Figure 8. Particle (electron, proton and antiproton) storage tests are planned in 1996-97.

References

[1]   M.H. Holzscheiter, "Antihydrogen Production and Spectroscopy," paper given at this workshop.
[2]   H. Kalinowsky, "LEAR Experiment PS196: CPT Tests with Antiprotons," paper given at this workshop.
[3]   T.W. Haensch and C. Zimmerman, Hyp. Int. 76 (1993) 47.
[4]   M. Mandelkern, Stanford Linear Accelerator Center report 23, no. 2 (1993) 15.
[5]   D.W. Townsend, CERN Courier 33, no.3 (1993) 1.
[6]   G. Jackson, "Antimatter Production Facility Concepts at Fermilab," paper presented at this workshop.
[7]   L. Krauss, "The Physics of Star Trek," Basic Books, (Harper Collins Publishers, Inc., 1995) p.92.
[8]   J.M. Sisterson, Nucl. Instrum. and Methods B99 (1995) 827.
[9]   T.E. Kalogeropoulos and R. Muratore, Nucl. Instrum. and Methods B40/41 (1989) 1322.
[10] A.H. Sullivan, Phys. Med. Biol. 30, no.12 (1985) 1297.
[11] A.J. Lennox, Ann. Rev. Nucl. and Part. Sci., 44 (1994) 155.
[12] U. Schneider and E. Pedroni, Med. Phys. 22, no. 4 (1995) 353.
[13] U. Oelfke, G.K.Y. Lam and M.S. Atkins, Phys. Med. Biol. 41 (1996) 177.
[14] M.V. Hynes, Physica Scripta T22 (1988) 195.